# Room Temperature Optically Pumped 2.56-$\mu$m Lasers With "W" Type InGaAs/GaAsSb Quantum Wells on InP Substrates

Chien-Hung Pan, Chia-Hao Chang, and Chien-Ping Lee, *Fellow, IEEE*

***Abstract*— The optically pumped laser using InGaAs/GaAsSb W-type quantum wells is demonstrated with a threshold power density ~40 kW/cm$^2$. The L–L curve and the dramatic line width shrinkage above threshold confirm, for the first time, mid-infrared lasing in this structure on InP substrates. The lasing wavelength at 2.56 $\mu$m is the longest lasing wavelength at room temperature for the interband transition of InP-based material system.**

***Index Terms*— InP-based, midinfrared lasers, optically pumped, type-II "W" type quantum wells.**

## I. Introduction

MIDINFRARED (mid-IR) lasers with wavelengths longer than 2 $\mu$m have applications in many different areas such as environmental monitoring, communications, life science, and molecular spectroscopy [1]. For the development of semiconductor mid-IR lasers, the InP substrate is a suitable platform due to its well established process technology, better wafer quality and lower cost compared to the conventionally used InAs and GaSb substrates. InAs/InGaAs type-I quantum wells (QWs) have been used to realize mid-infrared lasers on InP substrates [2]. However, it is difficult to extend the lasing wavelength beyond ~2.3$\mu$m due to the highly-strained structures. The "W" type QWs with the type II staggered band alignment using InGaAs/GaAsSb have been shown to be able to extend the lasing wavelength in the midinfrared range [3]. The high In-content and dilute nitride InGaNAs/GaAsSb type-II "W" QWs have also been designed and employed for the 1.55$\mu$m light emitting on GaAs substrates, and have been proposed for mid-IR lasers on InP substrates [4]–[9]. But most of mid-IR lasers were done on the lattice matched system using InAs/InGaSb structures on GaSb substrates [10]–[12]. In our previous study, we have obtained intense mid-IR photoluminescence from samples with properly designed "W" type QWs on InP substrates [13]. In this letter, for the first time, we successfully demonstrated the room temperature optically-pumped mid-IR lasers with the emission wavelength up to 2.56 $\mu$m on InP substrates using InGaAs/GaAsSb "W" type QWs.

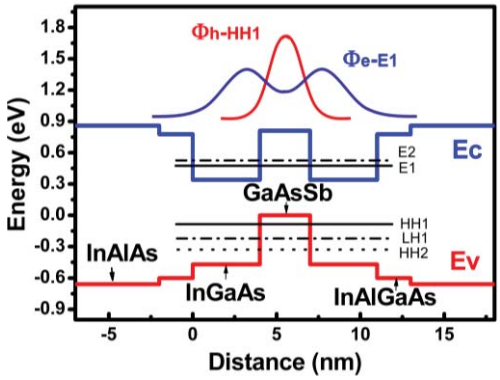


Fig. 1. Energy band diagram of the "W" type QW with the wavefunctions for lowest quantized electron (E1) state and hole (HH1) state.

The "W" structure consists of symmetric InGaAs/ GaAsSb/ InGaAs layers, which are sandwiched between In(Ga)AlAs barrier layers. The "W" band alignment, named from the shape of the conduction band profile, along with the electron and hole wavefunctions for our samples are illustrated in Fig. 1. Because of the type-II band alignment, the hole wavefunction is confined inside the GaAsSb QW; while the electron wavefunction is located in the two adjacent but coupled InGaAs QWs, which have the split symmetric (E1) and anti-symmetric (E2) states. This band alignment allows a smaller optical transition energy than the bandgap energies of the constituent layers, and therefore giving a longer emission wavelength. A general problem in the type-II structures is the small electron-hole wavefunction overlap, which results in a lower optical transition rate. This adverse effect, however, can be greatly reduced by using properly designed barrier layers in the "W" structure to provide quantum confinement for the electrons. The "W" structure preserves the two dimensional densities of states for both carries, and the type II configuration suppresses the Auger recombination [10], [14].

The samples used in this letter were grown on S-doped (001) InP substrates by a Veeco GEN ‖ molecular beam epitaxy system equipped with needle valve controlled As and Sb cracking cells. The group V species of $As_2$ and $Sb_2$ were used during the growth process. The active region of the laser diode had 15 stacks of the "W" QWs with each consisting

Manuscript received December 8, 2011; revised April 22, 2012; accepted April 23, 2012. Date of publication May 1, 2012; date of current version May 25, 2012. This work was supported in part by the National Science Council under Contract NSC99-2221-E-009-079-MY3, in part by the Center for Nano Science and Technology of National Chiao Tung University, in part by the National Nano Device Laboratories, and in part by the Aim for the Top University Plan of National Chiao Tung University, Taiwan.

The authors are with the Department of Electronics Engineering, National Chiao Tung University, Hsinchu 300, Taiwan (e-mail: panjoan.ee95g@g2.nctu.edu.tw; chiahao.ee96g@nctu.edu.tw; cplee@mail.nctu.edu.tw).

Color versions of one or more of the figures in this letter are available online at http://ieeexplore.ieee.org.

Digital Object Identifier 10.1109/LPT.2012.2197193

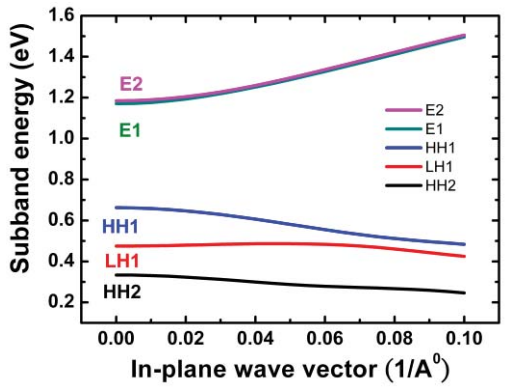


Fig. 2. Band structure of the designed "W" type QW based on the 8-band $k.p$ model.

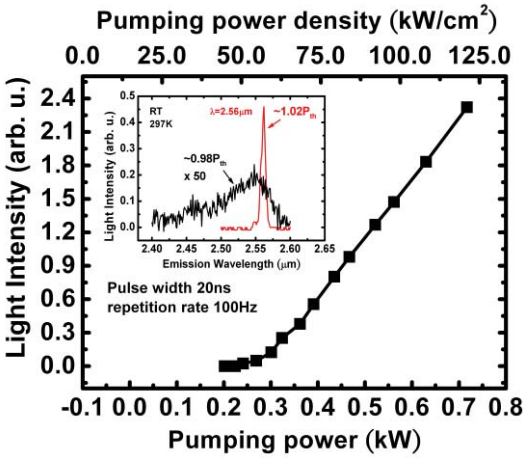


Fig. 3. L–L curve of a 1-mm-long "W" type laser at room temperature. The inset figure is the lasing spectra at ~0.98 $P_{th}$ (intensity 50x) and ~1.02 $P_{th}$.

of a symmetric $In_{0.53}Ga_{0.47}As/GaAs_{0.25}Sb_{0.75}/In_{0.53}Ga_{0.47}As$ (4/3/4nm) structure sandwiched between two 2 nm $In_{0.36}Al_{0.32}Ga_{0.32}As$ strain-compensated layers. The stacks were separated by 5 nm $In_{0.52}Al_{0.48}As$ barrier layers. The active region had a total thickness of ~300nm and was grown at 460 °C. The bottom and top optical cladding layers were made of lattice-matched $In_{0.52}Al_{0.48}As$ grown at 500 °C. Taking advantage of the lower refractive index of the InP substrate, only 0.3$\mu$m bottom cladding layer was used. The top cladding layer had a thickness of 2.25 $\mu$m and was capped by a 100 nm $In_{0.53}Ga_{0.47}As$ layer.

We have theoretically calculated the band structure of our "W" type QW using an 8-band $k.p$ theory. The result is shown in Fig. 2. The material parameters used in the calculation were taken from the published literature [15]. Based on the calculation, the effective band gap is found to be ~0.51eV. Because of the coupling between the two InGaAs electron QWs, there is a small energy splitting of ~17meV between the symmetric E1 and the anti-symmetric E2 bands at the Brillouin zone center. The energy separation between the first heavy hole (HH1) band and the first light hole (LH1) band, however, has a large value of ~188 meV, which is due to the small width of the hole QW and the large valence band offset of the InGaAs/GaAsSb type-II structure. The calculated wave function overlap between E1and HH1 is 0.27, and the overlap between E2 and HH1 is zero due to the anti-symmetric nature of the E2 wavefunction. The in-plane effective masses determined via parabolic curve fitting are $0.075m_0$ for the E1 band edge and $0.103m_0$ for the HH1 band edge at the zone center. The greatly reduced heavy hole effective mass is attributed to the compressively strained GaAsSb layer. This could lead to a lower transparency carrier density and a higher differential gain for the laser operation.

The sample was cleaved to form a 1 mm long cavity and optically pumped by a 1064nm (~1.2eV) pulsed fiber laser shaped via two cylindrical lenses, resulting in a beam size of ~ 200$\mu$m (width) x 3mm (length). The long axis of the pump beam was aligned in parallel with the cavity direction. The pumping light penetrated the thick InAlAs (~1.5eV) cladding layer and was absorbed by the active region. Using separate measurements of the transmission and reflection of samples with and without the epilayers, we estimated that around 25% of the pumping light was absorbed by the active region. The 15 stacks of "W" QWs also form an optical waveguide for the laser cavity. The light output from the cleaved mirror went through a long-pass filter and two focusing lenses. It then was dispersed through a monochromator and detected by a thermal electric cooled InGaAsSb photodetector. The room temperature lasing behavior is shown in Fig. 3. The L-L curve was measured under pulsed operation with 20 ns pumping pulses at a 100 Hz repetition rate. The lasing phenomenon is confirmed by the dramatically increased output power as well as the abruptly shrunk spectrum after a threshold power density ($P_{th}$) of ~40 kW/cm$^2$. Taking into account of the surface reflection and the percentage of the power absorbed, the absorbed threshold power density per well is ~0.467kW/cm$^2$. The spectra at $0.98P_{th}$ and $1.02P_{th}$ are shown in the inset of Fig. 3. The lasing wavelength is at 2.56 $\mu$m corresponding to the transition between the lowest E1 state and the first quantized heavy hole state (HH1). We have measured L-L curves of lasers with different cavity length (L) to extract internal loss ($\alpha i$), which is around 10.7cm$^{-1}$ at room temperature.

In order to further characterize our laser, we have measured the lasing performance at different temperatures. The temperature dependent L-L curves are plotted in Fig. 4. The extracted $P_{th}$ as a function of temperature is shown in the inset (in log scale). It is found that the slope efficiency hardly changes for temperatures below 250K. The slowly increased $P_{th}$ from 78K to 250K has a exponentially fitted characteristic temperature ($T_0$) of 487.8K. However, when the temperature is increased above 250K, the slope efficiency decreases and the threshold power increases at a much faster rate. The characteristic temperature is 41.8K when the temperature goes beyond 250K. It is known that the monomolecular (Shockley-Read) recombination and the radiative recombination are dominating processes at low temperatures. But they could not lead this $T_0$ change behavior because the Shockley-Read coefficient varies with $\sim T^{1/2}$ and the radiative coefficient gradually decays with T. The leakages of escaped carriers should also not play a role here since both the E1 level in the conduction

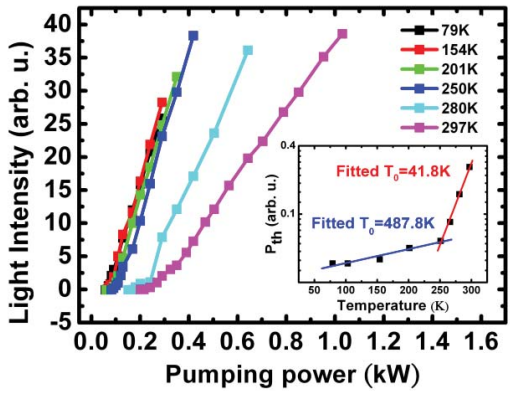


Fig. 4. L–L curves measured at different temperatures. The inset shows the plot of $P_{th}$ as a function of temperature.

band and the HH1 level in the valence band are more than 300meV deep compared to the surrounding potential barriers. The most probable reason for the rapid increase of threshold power density after ~250K is the Auger processes. The amount of the Auger effect for our laser is analyzed in the following.

We first calculated the laser's modal gain as a function of carrier density for a single "W" quantum well using the 8–band $k.p$ method including a Lorenzian line broadening function. The theoretically obtained 2D transparency carrier density was $\sim 1.1\times10^{12}\text{cm}^{-2}$. Based on the measured internal loss and the calculated modal gain, we estimated a 2D threshold density $\sim 1.6\times10^{12}\text{cm}^{-2}$ per well at room temperature. Since multiple quantum wells have higher optical gain and a larger optical confinement factor, the threshold carrier density should be lower than this number. Taking $N_{th} = 1.1\sim1.6\times10^{12}\text{cm}^{-3}$, we can estimate the carrier life time ($\tau_{th}$) at threshold using the relation, $\tau_{th} \approx N_{th}\hbar\omega_p/P_{th}f_{ab}(1\text{-}R)$, where $N_{th}$, $\hbar\omega_p$, $f_{ab}$, and R refer to the 2D threshold current density, the photon energy of the pump beam, the absorbed fraction, and the surface reflectivity, respectively. The obtained $\tau_{th}$ is in the range of 0.44~0.64 ns. This will lead to an Auger coefficient, $\gamma\, 3\sim1\tau_{th}\ (N_{th}/d)^2$, in the range of $1.37\sim4.21\times10^{-27}$ $\text{cm}^6/\text{s}$ at room temperature, where d of 15nm is used here for the thickness of one period "W" QW. This relatively high Auger coefficient explains why $T_0$ goes down at high temperatures. The value obtained is comparable to those in InAs/InGaSb type-II quantum wells on GaSb substrate, which also show similar $T_0$ at room temperatures [10], [14].

## II. Conclusion

In conclusion, for the first time we have demonstrated the room temperature optically-pumped mid-IR "W" type lasers on InP substrates. The lasing wave length is 2.56 $\mu$m with a threshold pumping power density of ~40kW/cm$^2$. The laser shows a characteristic temperature ($T_0$) of 487.8K when it is operated below 250K and a $T_0$ of 41.8K near room temperature. The small $T_0$ at room temperature is considered due to the dominated Auger processes. An Auger coefficient in the range of $1.37\sim4.21\times10^{-27}$ $\text{cm}^6/\text{s}$ was estimated. More studies are needed to improve the laser performance. We believe that the "W" structure on InP substrates are promising for the fabrication of mid-IR optoelectronics devices.

## References

[1] U. Willer, M. Saraji, A. Khorsandi, P. Geiser, and W. Schade, "Near-and mid-infrared laser monitoring of industrial processes, environment and security applications," *Opt. Lasers Eng.*, vol. 44, no. 7, pp. 699–710, 2006.

[2] T. Sato, M. Mitsuhara, N. Nunoya, T. Fujisawa, F. Kano, and Y. Kondo, "2.33 $\mu$m-wavelength distributed feedback lasers with InAs-$In_{0.53}Ga_{0.47}As$ multiple-quantum wells on InP substrates," *IEEE Photon. Technol. Lett.*, vol. 20, no. 12, pp. 1045–1047, Jun. 15, 2008.

[3] J. Y. T. Huang, *et al.*, "Design and characterization of strained InGaAs/GaAsSb type-II 'W' quantum wells on InP substrates for mid-IR emission," *J. Phys. D, Appl. Phys.*, vol. 42, no. 2, pp. 025108-1–025108-8, 2009.

[4] I. Vurgaftman, J. R. Meyer, N. Tansu, and L. J. Mawst, "(In)GaAsN-GaAsSb type-II 'W' quantum-well lasers for emission at $\lambda = 1.55$ $\mu$m," *Appl. Phys. Lett.*, vol. 83, no. 14, pp. 2742–2744, Oct. 2003.

[5] N. Tansu and L. J. Mawst, "Design analysis of 1550-nm GaAsSb-(In)GaAsN type-II quantum-well laser active regions," *IEEE J. Quantum Electron.*, vol. 39, no. 10, pp. 1205–1210, Oct. 2003.

[6] I. Vurgaftman, J. R. Meyer, N. Tansu, and L. J. Mawst, "InP-based dilutenitride mid-infrared type-II 'W' quantum-well lasers," *J. Appl. Phys.*, vol. 96, no. 8, pp. 4653–4655, Oct. 2004.

[7] J.-Y. Yeh, *et al.*, "Long wavelength emission of InGaAsN/GaAsSb type II 'W' quantum wells," *Appl. Phys. Lett.*, vol. 88, no. 5, pp. 051115-1–051115-5, Jan. 2006.

[8] J.-Y. Yeha, *et al.*, "Characteristics of InGaAsN-GaAsSb type-II 'W' quantum wells," *J. Cryst. Growth*, vol. 287, no. 2, pp. 615–619, 2006.

[9] L. J. Mawst, *et al.*, "MOCVD-grown dilute nitride type II quantum wells," *IEEE J. Sel. Topics Quantum Electron.*, vol. 14, no. 4, pp. 979–991, Jul./Aug. 2008.

[10] C. L. Felix, *et al.*, "High-temperature 4.5 $\mu$m type-II quantum-well laser with Auger suppression," *IEEE Photon. Technol. Lett.*, vol. 9, no. 6, pp. 734–736, Jun. 1997.

[11] W. W. Bewley, *et al.*, "Room-temperature 'W' diode lasers emitting at $\lambda \approx 4.0$ $\mu$m," *Appl. Phys. Lett.*, vol. 85, no. 23, pp. 5544–5546, 2004.

[12] C. L. Canedy, *et al.*, "High-power continuous-wave midinfrared type-II 'W' diode lasers," *Appl. Phys. Lett.*, vol. 86, no. 21, pp. 211105–211104, 2005.

[13] C. H. Pan, S. D. Lin, and C. P. Lee, "2–3 $\mu$m mid infrared light sources using InGaAs/GaAsSb 'W' type quantum wells on InP substrates," *J. Appl. Phys.*, vol. 108, no. 10, pp. 103105–103109, 2010.

[14] J. R. Meyer, *et al.*, "Auger coefficient in type-II InAs/$Ga_{1-x}In_xSb$ quantum wells," *Appl. Phys. Lett.*, vol. 73, no. 20, pp. 2857–2859, 1998.

[15] I. Vurgaftman, J. Meyer, and L. Ram-Mohan, "Band parameters for III–V compound semiconductors and their alloys," *J. Appl. Phys.*, vol. 89, no. 11, pp. 5815–5875, 2001.